Probing the Friedmann equation during recombination with future cosmic microwave background experiments

Oliver Zahn*
Fakultät für Physik, Ludwig-Maximilians-Universität, Geschwister-Scholl-Platz 1, 80799 München, Germany,
Max-Planck-Institut für Astrophysik, P.O. Box 1317, 85741 Garching, Germany,
and Department of Physics, New York University, 4 Washington Place, New York, New York 10003

Matias Zaldarriaga†
Department of Physics, New York University, 4 Washington Place, New York, New York 10003
and Institute for Advanced Study, Einstein Drive, Princeton, New Jersey 08540
(Received 16 December 2002; revised manuscript received 19 February 2003; published 18 March 2003)

We show that by combining measurements of the temperature and polarization anisotropies of the cosmic microwave background (CMB), future experiments will tightly constrain the expansion rate of the universe during recombination. A change in the expansion rate modifies the way in which the recombination of hydrogen proceeds, altering the shape of the acoustic peaks and the level of CMB polarization. The proposed test is similar in spirit to the examination of abundances of light elements produced during big bang nucleosynthesis and it constitutes a way to study possible departures from standard recombination. For simplicity we parametrize the change in the Friedmann equation by changing the gravitational constant G. The main effect on the temperature power spectrum is a change in the degree of damping of the acoustic peaks on small angular scales. The effect can be compensated by a change in the shape of the primordial power spectrum. We show that this degeneracy between the expansion rate and the primordial spectrum can be broken by measuring CMB polarization. In particular we show that the MAP satellite could obtain a constraint for the expansion rate H during recombination of $\delta H/H \simeq 0.09$ or $\delta G/G \simeq 0.18$ after observing for four years, whereas Planck could obtain $\delta H/H \leqslant 0.014$ or $\delta G/G \leqslant 0.028$ within two years, even after allowing for further freedom in the shape of the power spectrum of primordial fluctuations.

DOI: 10.1103/PhysRevD.67.063002 PACS number(s): 98.70.Vc, 98.80.Es, 98.80.Ft

I. INTRODUCTION

The parameters of our cosmological model will be determined with great accuracy by upcoming data from cosmic microwave background (CMB) experiments, galaxy surveys, weak lensing surveys, Lyman alpha forest studies, and other observations. With the new data it will be possible to perform a number of consistency checks that will strengthen our confidence in the underlying model. Some of these consistency checks have already been performed with existing data. Recent analyses of the CMB data have resulted in constraints on the baryon density $\Omega_b h^2$ that are in excellent agreement with its determination based on the study of the primordial abundances of light elements (e.g. [1,2]). The combination of CMB data with local measures of the Hubble constant [3] and measures of the local strength of galaxy clustering result in a determination of the cosmological constant that is in good agreement with results from the study of the luminosity of distant supernovae (e.g. [4,5]). Recently also joint big bang nucleosynthesis and CMB constraints on different dark energy models have been discussed in [6].

One of the assumptions of the cosmological model that has been hard to test is the explicit validity of the Friedmann equation—the relation between the expansion rate of the universe and its matter content. The difficulty lies in finding an epoch in the evolution of the universe during which both the energy density and the expansion rate can be determined independently. The two obvious candidates are the present time and big bang nucleosynthesis (BBN).

Precise measures of both the expansion rate and the matter density in the local universe are difficult to accomplish and suffer from various systematic problems. At present the expansion rate has been measured with errors on the order of 10% [3]. Direct determinations of the matter density however are more uncertain. It is fair to say that the general conclusion from these studies is that the Friedmann equation only holds true if either a cosmological constant or a curvature term is added. This is because direct determinations of the present matter density almost always point to $\Omega_m < 1$ (e.g. see [5]). Neither the cosmological constant nor the curvature scale can be constrained independently, that is without going through the Friedmann equation, so at best we can say that the Friedmann equation has not been tested accurately at the present epoch. A more radical interpretation would be that the Friedmann equation has been tested but that the test has failed. Although we do not support this interpretation, at present some infrared modification of gravity cannot be ruled out observationally. Such modifications are being explored for example as ways to solve the cosmological constant problem (see for example [7]) or to explain the accelerated expansion inferred from the luminosity distance to high redshift supernovae without resorting in a cosmological constant or a quintessence field (e.g. see [8,9]).

*Email address: zahn@mpa-garching.mpg.de
†Email address: mz31@nyu.edu

During the epoch of big bang nucleosynthesis (BBN) the situation is more fortunate. The energy density is dominated by radiation which we think we can estimate accurately. On the other hand the expansion rate affects the freeze-out abundances of light elements, so that a precision test of the Friedmann equation can be performed. The standard procedure is to constrain the number of relativistic degrees of freedom, g_*, which can be translated into a limit on the number of neutrino species. A lot of progress has been made in determining the primordial abundances. Recently the deuterium abundance in hydrogen clouds at high redshift was accurately determined [10–12]. Building on a prior of $N_\nu \geqslant 3$ these data have been exploited to enforce an upper limit of 3.2 at 2σ for the number of neutrino species, based purely on BBN considerations [13].

Progress has also been made in appreciating the systematical uncertainties that impair the determination of primordial ^{4}He (see e.g. [14,15]). Built on the safely established abundance ranges for deuterium, helium and lithium, it can be shown that the uncertainty in the number of relativistic degrees of freedom during BBN is around 9% (68% C.L.) [16]. This constraint can equally well be phrased as a constraint on the validity of the Friedmann equation: during nucleosynthesis the ratio of the squared expansion rate to the energy density can depart by only 9% from what is predicted by the Friedmann equation. Constraints on the expansion history during BBN have also been established in [17].

In this paper we propose using the anisotropies in the CMB to perform a test similar to the one that has been done using BBN. We will show that such a test can ultimately constrain the validity of the Friedmann equation during recombination more accurately than what has so far been reached within nucleosynthesis, albeit in a more model dependent way.

During recombination, the energy density is dominated by the density of non-relativistic matter which we cannot estimate directly. However the dark matter energy density enters in two different ways and one can exploit this to simultaneously determine the dark matter density and the expansion rate during recombination.

The ratio of matter to radiation energy density sets the redshift of matter radiation equality. At that time the expansion rate changes from a scaling as $t^{1/2}$ to $t^{2/3}$. Perturbation modes of the photon-baryon fluid that entered the horizon during the radiation dominated era behave differently than those that entered during the matter dominated era. Modes that entered during radiation domination provided the dominant contribution to the total density perturbation that generated the gravitational potential. On the contrary modes that entered the horizon during matter domination, were subdominant in their contribution to the total density perturbation which was dominated by the dark matter fluctuations. The gravitational potential acts as a source for perturbations in the photon baryon fluid. As a result, small scale modes that entered the horizon in the radiation era go through a sort of feedback loop that increases their amplitude as they cross the horizon (for a review of CMB physics see for example [18]). The anisotropy power spectrum is very sensitive to the redshift of matter radiation equality and thus the CMB should very accurately determine the ratio of dark matter to radiation energy density, i.e. the parameter $\Omega_m h^2$.

The dark matter density dominates over other energy components in the Friedmann equation during recombination. In the standard scenario, it sets both the redshift at which matter and radiation become equal and the rate of expansion during recombination through the Friedmann equation. In this paper we break the link between energy density and expansion rate by introducing a free parameter to modify the Friedmann equation. We investigate how well such a parameter can be constrained.

From a pragmatic perspective our study can be regarded as the investigation of a particular departure from standard recombination. Different variations have been studied in the literature. For instance the possibility that energetic sources of Ly-α- photons could be present during recombination to delay it was considered in [19]. Also, the possiblility of a time variation of the fine structure constant was investigated [20–22]. In [23] the effects of a time dependence of the gravitational constant have been outlined. The conclusion of these investigations and ours is that with future CMB data departures from standard recombination will be severely constrained and perhaps modifications that point to interesting new physics could be discovered.

In Sec. II, we will introduce our model and in Sec. III we will investigate the constraints that can be set with currently available data and forecast what future CMB experiments might be able to achieve. We will conclude in Sec. IV with discussion.

II. THE MODEL: VARIATION OF THE GRAVITATIONAL CONSTANT

In this section we introduce the model we will use to investigate how well one can test the Friedmann equation using the CMB. The problem is somewhat more subtle than in the case of BBN because we are dealing with the dynamics of perturbations that could be affected by the ''new physics'' in ways other than through a change in the expansion rate. Thus we need to find a self-consistent way of modifying both the dynamics of the universe and that of the perturbations.

One possibility is to add another component that contributes to the energy density during recombination, increasing the rate of expansion at that time. The additional component could be a quintessence field with a potential and initial conditions tuned so that it has some effect during recombination and is unimportant or only marginally important at other times (except perhaps today when it could start to dominate). This approach has the virtue of only modifying the expansion rate but it introduces too much freedom because results depend on when exactly this extra component is important. In such a model we also expect the ratio of the sound horizon at recombination to the angular diameter distance to the last scattering surface to change and thus that the acoustic peaks be slightly shifted. At late times the evolution of the gravitational potentials will also induce an integrated Sachs-Wolfe (ISW) effect. As a result, constraints on any specific model of this kind will come from these three effects [24].

In our study we want to isolate the information encoded in the change of the expansion rate at recombination so we will use a simpler prescription and assume that the gravitational constant G is somewhat different from its locally measured value. We introduce a single parameter λ such that

$$G \to \lambda^2 G. \tag{1}$$

The expansion rate is proportional to λ. With this prescription not only the Friedmann equation gets modified but also the dynamics of the perturbations changes because it depends on the strength of gravity. We will show in the following that our prescription has the nice feature that it only changes the CMB power spectrum through the change in recombination, allowing us to isolate the observable effects of this change. The basic reason is that gravity does not have a preferred scale and that we only measure angles when studying the CMB. If G were slightly different all that would happen is that the universe would be expanding a bit faster or slower by a factor λ so that the ''expansion clock'' would be running at a different rate. Such a change cancels in the ratios of distances that we measure with the CMB. The only way we can find out that such an alteration had occurred is by having an independent clock that measures the expansion rate. In our case this independent clock will be the physics of hydrogen recombination. In this sense our simple test is very similar to what has been done in the context of BBN.

Effect of λ on the CMB anisotropies

The dependence of the Hubble parameter and the dynamics of perturbations on the gravitational constant will lead to modifications of the CMB anisotropies as we vary the parameter λ. We will discuss the physics in this section.

We start by considering the modification to the Friedmann equation,

$$H^2 = \left(\frac{\dot{a}}{a}\right)^2 = \frac{8\pi}{3} G\rho \to \frac{8\pi}{3}\lambda^2 G\rho \tag{2}$$

where ρ is the total energy density. As a function of the expansion factor a and λ, the expansion rate H satisfies

$$H(a,\lambda) = \lambda f(a), \tag{3}$$

where the function $f(a)$ is independent of λ. Thus with this simple prescription, the shape of the function H of a is not changed by λ, only the amplitude changes. For example the redshift at which matter and radiation contribute equally to the energy density does not change. The change introduced is a simple rescaling of the ''expansion rate clock.''

In order to understand how the anisotropies get modified, we start by writing down the integral solution for the temperature anisotropies produced by a mode of wave vector $\mathbf{k}$ observed towards direction $\hat{\mathbf{n}}$ [25]. The temperature can be written as an integral along the line of sight over sources,

$$\Delta T(\hat{\mathbf{n}},\mathbf{k}) = \int_0^{\tau_0} d\tau S(k,\tau) e^{i\mathbf{k}\cdot\hat{\mathbf{n}}D(\tau)} g(\tau). \tag{4}$$

In this equation $S(k,\tau)$ is the source term, $g(\tau)$ is the visibility function, and $D(\tau)$ is the distance from the observer to a point along the line of sight corresponding to the conformal time τ ($a d\tau = dt$). Dots indicate differentiation with respect to τ.

The visibility function $g(\tau)$ can be written in terms of the opacity for Thomson scattering κ as

$$g(\tau) = \dot{\kappa}\exp(-\kappa) = -d/d\tau \exp(-\kappa) \tag{5}$$

with

$$\kappa = \sigma_T \int_\tau^{\tau_0} a n_e(\tau) d\tau, \tag{6}$$

where σ_T is the Thomson scattering cross section and $n_e(\tau)$ is the number density of free electrons. We have also defined $\dot{\kappa} = \sigma_T a n_e$. Finally, the source term in the integral equation is given by

$$S = \phi + \frac{\delta_\gamma}{4} + \hat{n}\cdot\mathbf{v}_b \tag{7}$$

where ϕ is the gravitational potential, δ_γ is the fractional perturbation in the photon energy density and $\mathbf{v}_b$ is the baryon velocity.

The acoustic oscillations in the photon-baryon plasma satisfy (see e.g. [26])

$$\ddot{\delta}_\gamma + \frac{\dot{R}}{(1+R)}\dot{\delta}_\gamma + k^2 c_S^2 \delta_\gamma = 4\left[\ddot{\phi} + \frac{\dot{R}}{1+R}\dot{\phi} - \frac{1}{3}k^2\phi\right] \tag{8}$$

with the sound speed $c_S^2 = 1/3(1+R)$, and the baryon-photon momentum density ratio $R = (p_b + \rho_b)/(p_\gamma + \rho_\gamma) \simeq 3\rho_b/4\rho_\gamma$. The velocity satisfies

$$\dot{\delta}_\gamma + k v_\gamma + \dot{\phi} = 0. \tag{9}$$

Finally the gravitational potential satisfies the Poisson equation

$$-k^2\phi = 4\pi\lambda^2 G\rho\delta^{total}, \tag{10}$$

where $\rho\delta^{total}$ gives the combined perturbation due to all the fluids.

We are now ready to study the dependence of ΔT on λ. For this purpose it is best to consider the expansion factor as a time variable rather than τ. We note that

$$\frac{d}{d\tau} = \frac{da}{d\tau}\frac{d}{da} = a^2\cdot H\cdot\frac{d}{da} = \lambda f(a) a^2 \frac{d}{da}. \tag{11}$$

As a result, when we change time variables, every time derivative introduces a factor of λ. By inspection of Eqs. (8) and (10) it is clear that the dynamics of a mode with wave number k in a universe with $\lambda \neq 1$ is equivalent to the dynamics of a mode with $k' = k/\lambda$ in a universe with $\lambda = 1$. That is,

$$S(k,a,\lambda) = S(k/\lambda, a, \lambda = 1). \tag{12}$$

We have explicitly included the λ dependence of the source to make our argument clearer.

To obtain the CMB power spectrum, we first need to expand Eq. (4) in Legendre polynomials. The amplitude of the l expansion coefficient is

$$\Delta T_l(k,\lambda) = \int_0^1 da \tilde{S}(k,a,\lambda) j_l(kD(a,\lambda)) \tilde{g}(a,\lambda). \quad (13)$$

We have introduced $\tilde{g}(a,\lambda) = -d/da \exp(-\kappa)$. The conformal distance D is given by

$$D(a,\lambda) = \int_a^1 \frac{da}{H(a)a^2} = \lambda^{-1} D(a,\lambda=1). \quad (14)$$

Thus if the visibility function where to be independent of λ we would have

$$\Delta T_l(k,\lambda) = \Delta T_l(k/\lambda,\lambda=1). \quad (15)$$

The power spectrum is calculated from $\Delta T_l(k,\lambda)$ using

$$C_l(\lambda) = \int \frac{dk}{k} P(k) |\Delta_{Tl}(k,\lambda)|^2$$

$$= \int \frac{dk'}{k'} P(k'\lambda) |\Delta_{Tl}(k',\lambda=1)|^2, \quad (16)$$

where $P(k)$ is the power spectrum of primordial fluctuations which is usually taken to be a power law $P(k) \propto k^{n-1}$. Thus we see that provided we adjust the amplitude of the primordial power spectrum appropriately $C_l(\lambda) = C_l(\lambda=1)$.

Our result is qualitatively very easy to understand: gravity introduces no preferred scale, so the dynamics of the perturbations remains the same when scales are measured in units of the expansion time. As a result, the angular power spectrum does not change as we change λ.

Of course this conclusion only holds true if the visibility function is not affected by λ. However the physics of recombination does introduce a preferred timescale, so the power spectra of the anisotropies will actually change. In other words, in our simple minded prescription the only source of change is the difference in the way recombination proceeds as we change the expansion rate of the universe at recombination. This is the sense in which our model resembles the studies done in the context of big bang nucleosynthesis.

Let us now turn to study how the visibility function changes with λ. It depends on the ionization fraction $x_e = n_e/n_H$, where n_e again is the free electron density and n_H is the number density of hydrogen atoms. The evolution of the ionization fraction is modified when G is changed. It evolves according to (e.g. [27])

$$\frac{dx_e}{d\tau} = aC_r[\beta(T_b)(1-x_e) - n_H \alpha^{(2)}(T_b) x_e^2] \quad (17)$$

where $a(t)$ is just the scale factor, $\beta(T_b)$ is the collisional ionization rate from the ground state and $\alpha^{(2)}(T_b)$ is the recombination rate to excited states. The baryon temperature is T_b and the Peebles correction coefficient (which also depends on the expansion rate) is denoted C_r [28]. The transformation from τ to $a(\tau)$ as a time variable using Eq. (11), makes clear, that contrary to what happens to the perturbation equations, $x_e(a)$ depends on λ. We plotted x_e for different values of λ in Fig. 1. The behavior is easy to understand; the faster the universe is expanding at a given redshift (i.e. the larger the λ), the more difficult it is for hydrogen to recombine and hence the larger is x_e.

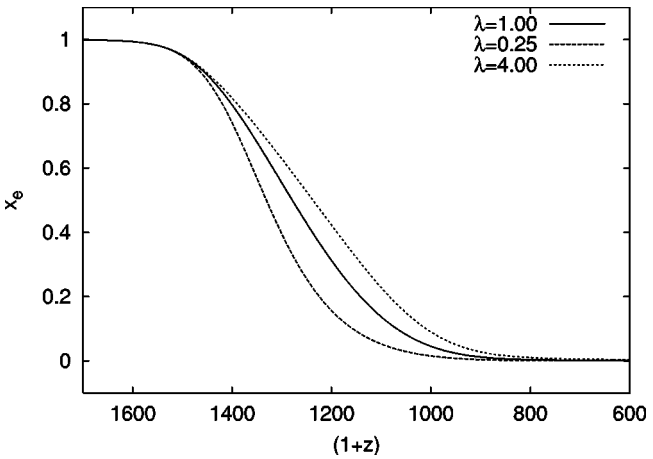

FIG. 1. Ionization fraction as a function of redshift for three values of $\lambda = 0.25,1,4$.

The change in x_e leads to a change in the visibility function which we show in Fig. 2. As λ is increased, the visibility function becomes broader. This broadening leads to a larger damping of the anisotropies on small (angular) scales, as shown in Fig. 3. We note however that even for a factor of four change in λ the changes in the visibility function are rather small. What happens is that if we increase λ, x_e at a given redshift after the start of recombination increases. However, when calculating optical depths this change almost exactly cancels with the decrease in the time intervals between different redshifts due to the increased expansion rate. As a result changes in both the location and shape of the

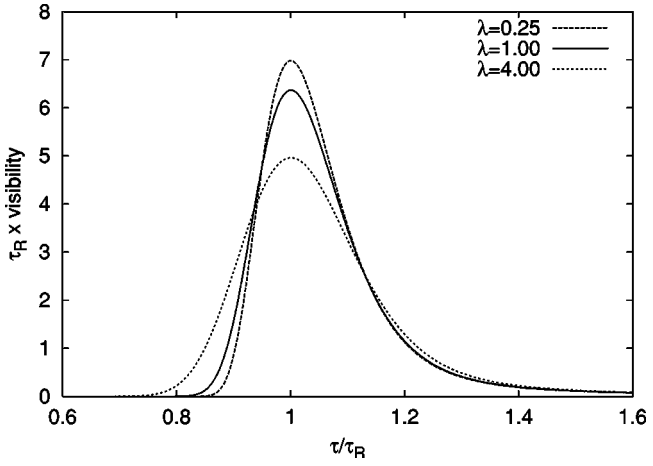

FIG. 2. The visibility function as a function of conformal time for $\lambda = 0.25,1,4$. The axes have been rescaled to take out the overall scaling of τ with λ.

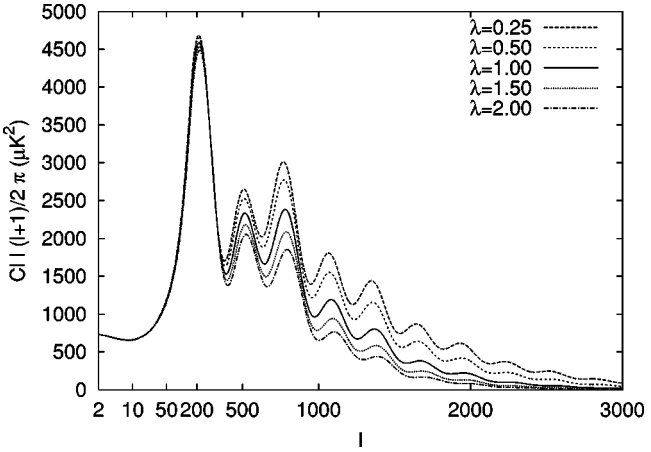

FIG. 3. Effect of λ on the temperature power spectrum: Higher peaks are more severely damped as λ increases while the height of the first peak is almost unchanged.

visibility function are small even for large changes in λ.

Figure 3 shows that the effect of λ is to change the relative amplitudes of the acoustic peaks on different scales. This effect can be compensated by changing the relative amplitude of modes of different scales in the primordial power spectrum.

We are now going to study what happens to CMB polarization and to show that it can lift the degeneracy between λ and the shape of the primordial power spectrum. To understand the effect of λ on the polarization we will employ the simple analytic expression for the amplitude of the Q Stokes parameter produced by a single Fourier mode k [29]:

$$Q \propto c_s k \delta\tau_D \sin(k c_S \tau_D) e^{-k^2/k_D^2} \tag{18}$$

where τ_D is the conformal time corresponding to the peak of the visibility function, $\delta\tau_D$ is its width and k_D describes the damping of the small scale modes. As we discussed above, the damping increases with the width of the visibility function, so the exponential factor will lead to the same effect we described for the temperature. The difference in the case of the polarization is the extra $\delta\tau_D$ in the amplitude of the polarization. This extra factor comes from the fact that if the visibility function is wider the photons will travel on average longer between their last two scatterings which will enhance the quadrupole anisotropy and will thus lead to a higher level of polarization [29]. For that reason, there exists a characteristic wavemode value k^*, for scales larger than which the polarization power spectrum will increase with λ, while it will decrease for scales smaller than k^*.

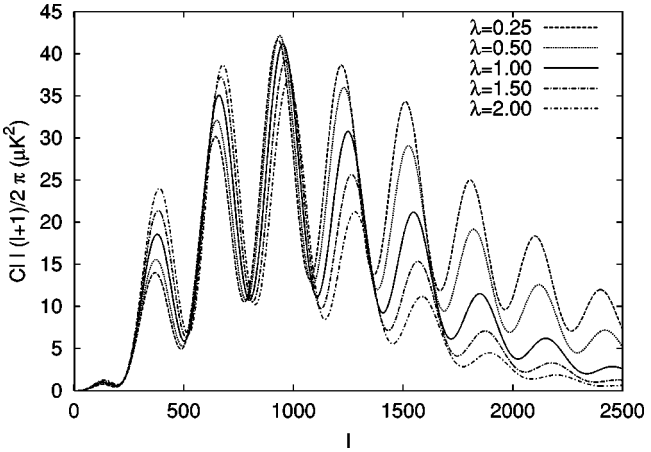

FIG. 4. The effect of λ on E-type polarization power spectra. On large angular scales the polarization signal will be boosted, while on small scales, it will be damped.

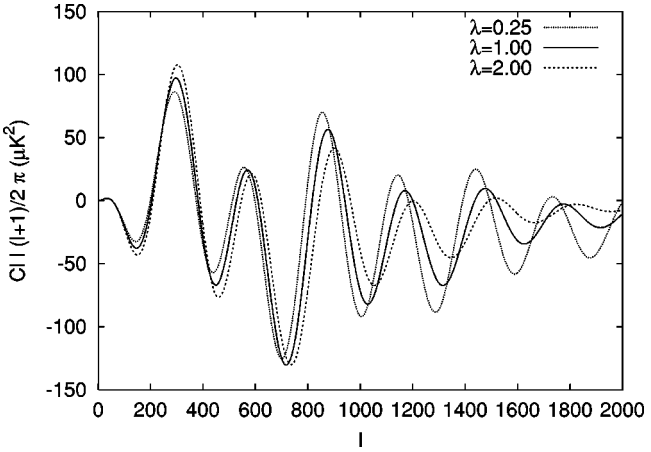

FIG. 5. The effect of λ on the cross correlation between temperature and E-type polarization.

The polarization power spectrum is plotted in Fig. 4. We see that for ls larger than around 800, the polarization behaves just as the temperature does, decreasing for increasing λ. On larger scales the effect is opposite, the amplitude of polarization relative to temperature roughly increases by 10% when λ increases by 20%. This response of the anisotropies on λ is what will help to break the degeneracy between λ and the primordial power spectrum when information from polarization is included.

For completeness we show the temperature polarization cross correlation power spectrum in Fig. 5. The cross correlation will be easier to detect in experiments such as the Microwave Anisotropy Probe (MAP) satellite where the ac-

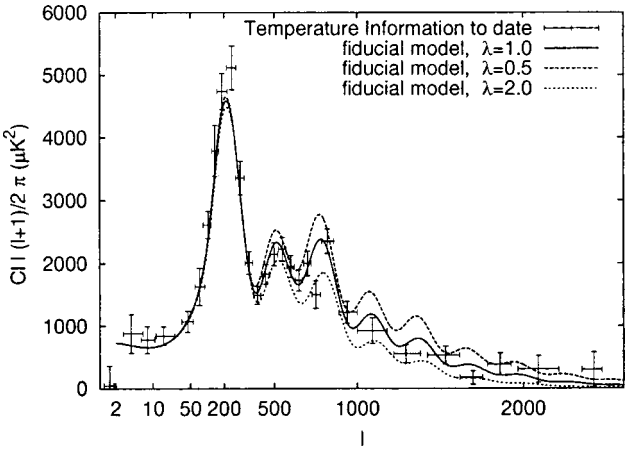

FIG. 6. Compilation of current CMB temperature anisotropy data; superimposed are three models with differing values of λ.

TABLE I. Mean value and standard deviation σ for the currently available temperature data.

Param.	Mean	σ_{Markov}
λ	1.749	0.471
n_S	1.038	0.0553

curacy of the polarization measurement is limited by detector noise. The cross correlation power spectrum behaves similarly to the polarization power spectrum; when λ is increased the power on small scales is suppressed while on large scales it is amplified.

III. CONSTRAINTS ON λ

In our likelihood analysis of currently available and simulated future data we let vary Ω_Λ, $\omega_{\text{dark matter}}=\Omega_{\text{dark matter}}h^2$, $\omega_{\text{baryon}}=\Omega_{\text{baryon}}h^2$, the optical depth due to reionization τ_{ri}, λ and the amplitude and shape of the primordial power spectrum. We explicitly assume that the universe is flat.

As we mention above, we expect there to be a degeneracy between the shape of the primordial power spectrum and the parameter λ. To study this effect in the case of future satellite missions which will measure polarization and could break this degeneracy, we introduce additional freedom in the shape of the spectrum. Rather than just assuming that $P(k)$ is of power law form

$$P(k)=k^{n-1}\Leftrightarrow\frac{\ln P(k)}{\ln(k)}=n-1, \tag{19}$$

we also allowed spectra with curvature by adding another term in the expansion of $\ln P$ as a function of $\ln k$,

$$\ln P(k)/P(k_0)=(n-1)\ln(k/k_0)+\alpha[\ln(k/k_0)]^2+\cdots \tag{20}$$

where k_0 is the pivot point. With this prescription the effective slope of the power spectrum changes slightly with scale,

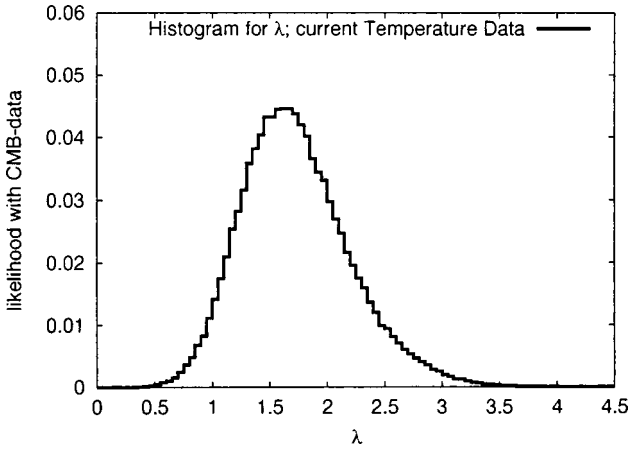

FIG. 7. Histogram for likelihood of λ given present CMB temperature anisotropy information.

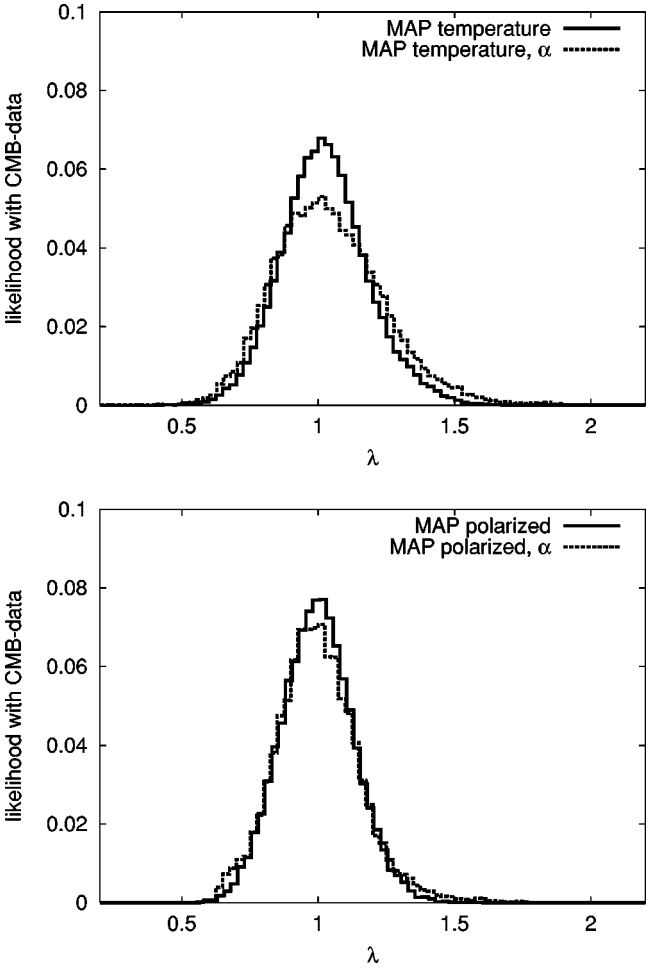

FIG. 8. Likelihood distributions of λ for a one year observation with MAP. Compared is the case in which one assumes a simple power law spectrum of the initial perturbations (solid lines) with the case in which one leaves further freedom to $P(k)$ (dashed lines). To obtain the figure on the top, only temperature information was used and for the one on the bottom polarization was included.

$$\frac{\partial\ln P(k)}{\partial\ln k}=n-1+\alpha\ln(k/k_0). \tag{21}$$

We employed two kinds of likelihood analysis. For an evaluation of what currently available data can tell us about λ we used an importance sampling Markov-chain method to generate a large number of cosmological models distributed according to the likelihood distribution $\mathcal{L}(\text{model}|\text{data})$. This is more efficient than an exploration of the entire parameter space, because the sampling is weighted and statistics can be established over the target distribution itself. Moreover the algorithm is very easy to implement. The weighted sampling is achieved through the Metropolis-Hastings algorithm. The application of the Markov method to the extraction of cosmological parameters from CMB information has been suggested in [30].

To speed up the power spectrum computations for the Markov chain we made use of the k-splitting technique discussed in [31]. For each model we marginalized analytically over the amplitude of the scalar fluctuations. In the end we

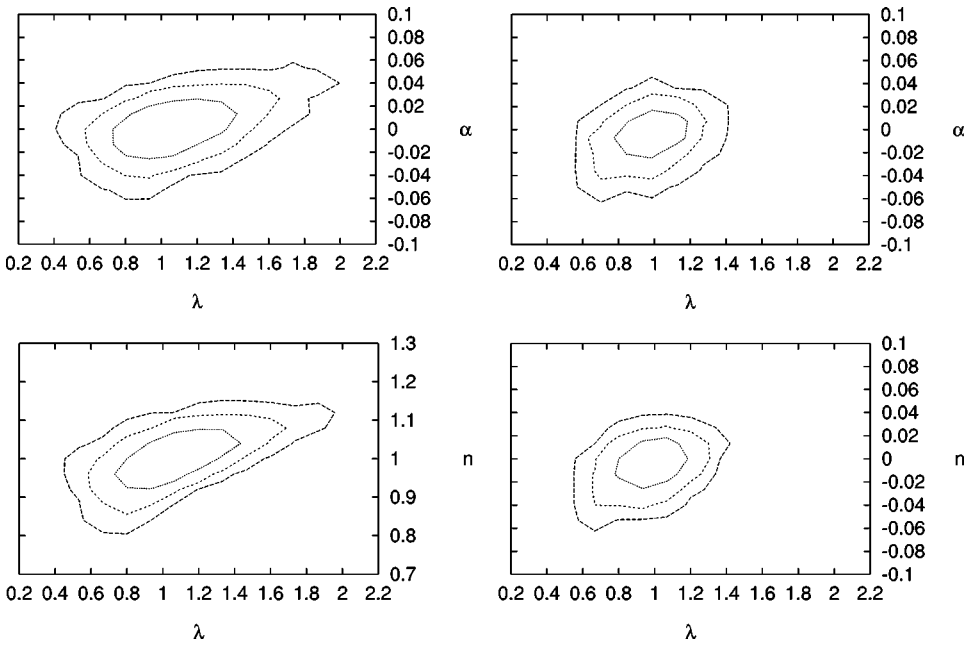

FIG. 9. We plot the 68.3,95.4 and 99.7% contour lines of 10^5 cosmological models of our Markov chains. The upper two plots show a projection onto the $\lambda-\alpha$ plane; the left plots are for temperature and the right ones include polarization information. The lower two plots show the degeneracy of λ with the slope of the spectrum of scalar perturbations, n_S. It can be seen in the upper and lower plots that polarization information reduces the degeneracy with the shape of the initial power spectrum.

constructed histograms and computed expectation values and variances for each parameter directly from the Markov chain.

In order to estimate what the satellite missions MAP and Planck will be able to tell us about the relation between the energy density and the expansion rate of the universe during recombination, we investigated the shape of the likelihood function $\mathcal{L}(C_l|\theta_i)$ (for a power spectrum C_l given a model consisting of the cosmological parameters θ_i) in the vicinity of its maximum directly by a Fisher matrix evaluation. This method has been widely used to make predictions for the errors that are to be expected in the extraction of cosmological parameters from planned CMB experiments. The Fisher matrix is given by the expectation value of the second derivative of the logarithm of the likelihood function $\mathcal{L}(C_l|\theta_i)$. Assuming Gaussianity of the likelihood it is of the form

$$F_{ij}=\sum_l \sum_{A,B} \frac{\partial C_{Al}}{\partial \theta_i}\mathbb{C}^{-1}(\hat{C}_{Al},\hat{C}_{Bl})\frac{\partial C_{Bl}}{\partial \theta_j}, \qquad (22)$$

where A and B run over the three observables: temperature, E-type polarization, T-E cross correlation and i,j run over the cosmological parameters. The covariance matrix between parameters is given by the inverse of the Fisher matrix. Overall we verified a good agreement between Fisher matrix and Markov chain results which confirms that the likelihood function $\mathcal{L}(C_l|\theta_i)$ resembles relatively well a Gaussian in the vicinity of its maximum value.

A. Constraints from currently available temperature data

In order to find the constraints which can be imposed on the parameter λ using available temperature data, we employed a compilation of 30 experiments which functions as a complete account of pre-MAP CMB temperature anisotropy information.[1] The data, which have been compressed to 29 bins, are plotted in Fig. 6. In this context, we actually assumed a simple power law behavior of the primordial scalar perturbations.

The results we obtained from the Markov-chain analysis are shown in Table I and Fig. 7. As expected from the rather weak dependence of the anisotropies on λ we find that current data cannot put severe constraints on the expansion rate during recombination even though other cosmological parameters are well determined.

Having emphasized the importance of measuring the linearly polarized component of the CMB, we should also note that its recent first detection by DASI [36], unfortunately has too large error bars to deliver much information about λ. Adding the DASI data in fact only changes the standard error in the determination of λ by 3%.

B. Future satellite missions and the relevance of measuring polarization

An up to date estimate of the expected angular resolutions and sensitivities of the MAP and Planck satellites has been obtained from the experimental groups websites. For both satellites we combined the three frequency channels with the highest angular resolution and took into account the number of polarized instruments. In the case of MAP the sensitivity estimate has been provided for 2 years of observation and the

[1]The results of the Archeops [32] and ACBAR experiments [33] as well as the new Boomerang data [34] were added to the compilation described in [35].

TABLE II. Fisher matrix results for MAP's expected 2 year data (in brackets are the values expected for a 4 year observation). The first two columns are the results when polarization information is not included. In the second column the curvature of the primordial spectrum was left to vary. In the last two columns polarization information was included.

T	$(F_{ii}^{-1})^{1/2}$	$(F_{ii}^{-1})^{1/2}$, α	$T+P$	$(F_{ii}^{-1})^{1/2}$	$(F_{ii}^{-1})^{1/2}$, α
λ	0.1928 (0.1279)	0.2616 (0.1992)	λ	0.1373 (0.0903)	0.1658 (0.1165)
n	0.0294 (0.0248)	0.0646 (0.0595)	n	0.0170 (0.0144)	0.0489 (0.0418)
α	$\times$	0.0237 (0.0222)	α	$\times$	0.0151 (0.0137)

angular resolutions $\theta_{\rm fwhm}$ are 13.2, 21.0 and 31.8 arcminutes for the three channels observing at 90, 60 and 40 GHz. This leads to a raw sensitivity of

$$w_T^{-1}=(0.081\ \ \mu\mathrm{K})^2$$

$$w_P^{-1}=(0.114\ \ \mu\mathrm{K})^2.$$

If MAP observes for four years the raw sensitivities (w^{-1}) will be halved. For the Planck satellite mission (here the sensitivity estimates are given for a one year observation period), the three channels (217, 143 and 100 GHz) at $\theta_{\rm fwhm}=5.0,7.1$ and 9.2 arcminutes give together

$$w_T^{-1}=(0.0084\ \ \mu\mathrm{K})^2$$

$$w_P^{-1}=(0.0200\ \ \mu\mathrm{K})^2.$$

Again the raw sensitivities for a two year observation will be half of these values. For both satellites, a sky coverage of $f_{Sky}=0.8$ was assumed.

From these experimental characteristics the full estimator covariance matrices for each multipole l can be constructed (e.g. [37]). The diagonal terms of the covariance matrices for temperature, polarization and cross correlation are

$$\mathrm{Cov}(\hat{C}_{Tl}^2)=\frac{2}{(2l+1)f_{Sky}}(C_{Tl}+w_T^{-1}B_l^{-2})^2 \tag{23}$$

$$\mathrm{Cov}(\hat{C}_{El}^2)=\frac{2}{(2l+1)f_{Sky}}(C_{El}+w_E^{-1}B_l^{-2})^2 \tag{24}$$

$$\mathrm{Cov}(\hat{C}_{Cl}^2)=\frac{1}{(2l+1)f_{Sky}}[C_{Cl}^2+(C_{Tl}+w_T^{-1}B_l^{-2})\times(C_{El}+w_P^{-1}B_l^{-2})] \tag{25}$$

where the beam window function $\mathcal{B}_l$ is to be constructed from the relevant frequency channels with their individual sensitivities w_c as

$$\mathcal{B}_l^2=\sum_c B_{l,c}^2\frac{w_c}{w} \tag{26}$$

$$B_{l,c}^2=e^{-l(l+1)\theta_b^2,c}. \tag{27}$$

Here, the standard width of the beam θ_b is obtained from the full width half maximum resolution by

$$\theta_b,c=\frac{\theta_{\rm fwhm,c}}{\sqrt{8\ln 2}}. \tag{28}$$

As a fiducial model we have adopted the parameter values

τ	Ω_K	Ω_Λ	$\omega_{\rm dm}$	$\omega_{\rm ba}$	n_S	λ
0.05	0	0.7	0.14	0.02	1	1

(29)

They imply a hubble constant of $h=0.73$.

1. Expected constraints from MAP

The analysis of expected constraints from the MAP satellite mission shows the constraints it can put on λ are rather weak. Better sensitivity is needed to accurately determine the polarization and higher angular resolution to map the damping tail. On the other hand our results illustrate how the inclusion of a curvature term for the primordial spectrum significantly weakens the constraints that one obtains from the temperature data.

A precision test of the Friedmann equation will have to wait until both polarization and the damping tail are measured accurately. In the near future experiments such as Boomerang, BICEP, Polatron and others are expected to significantly improve polarization measurements while CBI, ACBAR and others will map the damping tail. In a few more

TABLE III. Fisher matrix results for Planck's estimated 1 year data (brackets contain the 2 year results). Columns are equivalent to those in Table II.

T	$(F_{ii}^{-1})^{1/2}$	$(F_{ii}^{-1})^{1/2}$, α	$T+P$	$(F_{ii}^{-1})^{1/2}$	$(F_{ii}^{-1})^{1/2}$, α
λ	0.0170 (0.0152)	0.0325 (0.0278)	λ	0.0115 (0.0093)	0.0174 (0.0141)
n	0.0118 (0.0106)	0.0182 (0.0160)	n	0.0072 (0.0060)	0.0098 (0.0080)
α	$\times$	0.0072 (0.0620)	α	$\times$	0.0039 (0.0033)

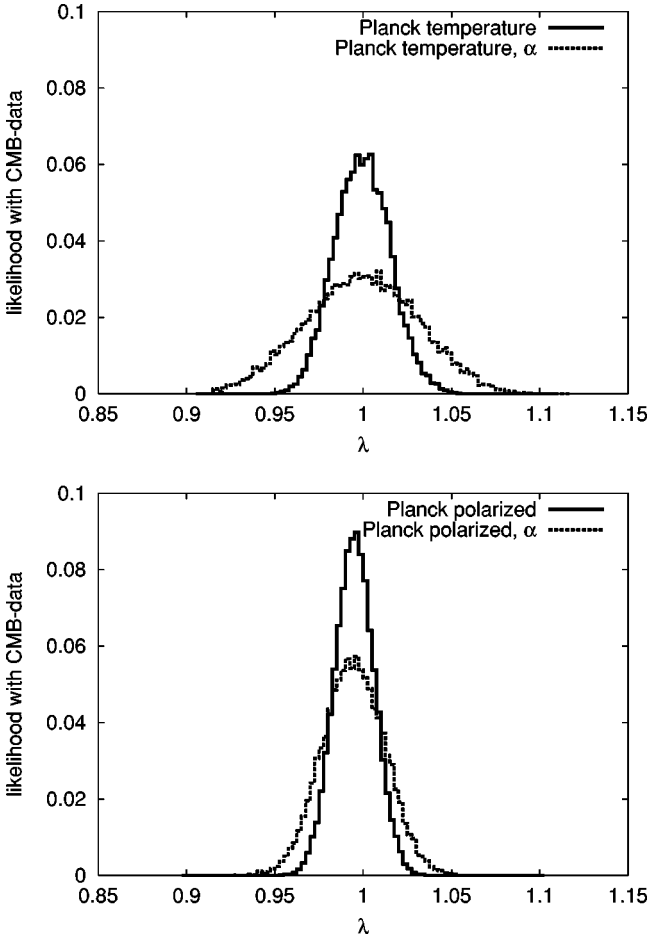

FIG. 10. The distribution of values of lambda for one versus two degrees of freedom in the primordial power spectrum. The upper plot shows the temperature case while the lower includes polarization.

years, the Planck satellite will measure both temperature and polarization accurately enough to severely constrain any change in λ. We will present an analysis of Planck's sensitivity in the next section.

In Sec. II we discussed the different response to a change of λ of the temperature and the polarization anisotropy. We found that on large angular scales polarization power is increased if we increase the expansion rate during recombination, while the temperature anisotropy is almost not affected on these scales. When only temperature is being measured, changes in the expansion rate of the universe during recombination are strongly degenerate with the slope of the spectrum of the initial scalar perturbations, which can be clearly seen in Figs. 8 and 9. Because polarization responds differently on different scales to a change of λ, it breaks this degeneracy. We show this in Fig. 9. The result of the likelihood analysis which includes polarization information is included in Table II.

We noticed that a major part of the information on λ from MAP's polarization measurements will come from the cross correlation between temperature and polarization. When adding just the cross correlation information we found that we gain almost 90% of the information that is gained in the case in which all three estimators are included.

2. Expected constraints from Planck

The Planck satellite explores the very small structures in the primeaval plasma in a multipole range up to nearly $l = 3000$. Even if only Planck's temperature data are used, the standard error in λ will after a one year observation be as small as 3.2%, even if one marginalizes over the parameters that describe the shape of the primordial power spectrum (Table III). This corresponds to a constraint on the gravitational constant of $\delta G/G = 0.064$. Finally, the improvement gained from Planck's polarization data

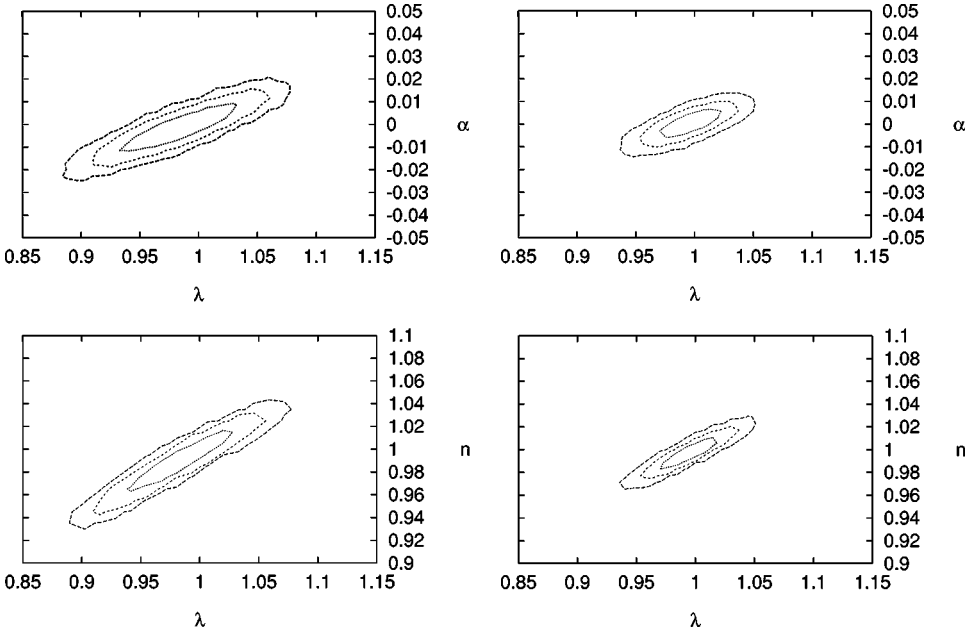

FIG. 11. Contour lines for the case of Planck (with the same ordering as above). Again it is shown that one can lift the degeneracy between λ and the shape of the primordial fluctuations by measuring CMB polarization.

($\delta\lambda/\lambda \simeq 0.017 \Leftrightarrow \delta G/G \simeq 0.034$) is shown on the right-hand side of that same table. If one assumes that there is no curvature in the primordial power spectrum the constraint on G would be as small as $\delta G/G = 1.8\%$ after an observation of two years. Figures 10 and 11 show again, analogously to the case of MAP, how polarization helps break the degeneracy between λ and the parameters that describe the shape of primodial perturbations.

We have extended our investigation beyond Planck to the case of an experiment which has essentially no noise and where the errors in the CMB power spectra are on all scales dominated by the cosmic variance term. For example experiments currently being considered for measuring the *B* modes of CMB polarization would be cosmic variance limited for E polarization over a wide range of l*s* (e.g. [38]). Such an optimal experiment, exploring structures into a multipole range of $l = 4000$, represents the limit of how much information on λ one could extract from the CMB in principle. We found an expected error for λ of order 0.3% which translates into a constraint of the value of the gravitational constant during recombination of $\delta G/G \simeq 0.6\%$.

IV. DISCUSSION

We have made the expansion rate of the universe a free parameter in a likelihood analysis within an eight-dimensional cosmological parameter space. For simplicity we assumed that the gravitational constant is changed by a factor λ. We showed that an increase of λ leads to a wider visibility function which in turn increases the damping of anisotropies on small scales and increases the level of large scale polarization.

We calculated the constraints that current CMB data can impose on the expansion rate. The constraints that can be imposed on the parameter λ using the information from the damping tail are severely weakened by our lack of knowledge about the shape of the primordial power spectrum. We showed that measuring polarization helps to break this degeneracy. Current data can only constrain λ to about 74% at 1σ. We showed that MAP could obtain 9% error bars for λ while for Planck error bars go down to 0.9%. We also explored the ultimate limit that could be achieved by a cosmic variance limited experiment measuring anisotropies up to $l = 4000$ and found errors of under a percent in that case. Thus next generation experiments should be able to deliver very accurate constraints on the expansion rate of the universe during recombination.

We acknowledge that if the variation of the gravitational constant during recombination is taken seriously a model needs to be built where *G* changes after recombination and converges towards the stable value observed in laboratory experiments today and where its current rate of change is less than the experimental bound $\dot{G}/G \simeq 10^{-12}\ \mathrm{yr}^{-1}$ [23,39]. If we introduce a scalar field to control the value of *G* we would also have to require that this field does not lead to an unacceptably large fifth force and does not violate solar system constraints such as shifting the orbit of the moon through the Nordvedt effect [40,41].

The shift of *G* after recombination will induce a change in the angular diameter distance to recombination, shifting the CMB power spectrum in *l*. We have shown that future experiments will be able to constrain the change of *G* to a few percent due to its effect at recombination. As a result the induced shift in the peak positions would be small and could be interpreted as slightly different values of Ω_m and/or Ω_Λ, the two parameters that control the distance to the last scattering surface in conventional models. In the same way, any induced integrated Sachs-Wolfe (ISW) effect would be difficult to observe because of the cosmic variance limitation. If observed with a high enough accuracy it should not be identical with what is predicted by a simple cosmological constant model.

In this paper we have shown that future measurements of the CMB anisotropy will be able to extract information about the relation between the expansion rate and the energy density of the universe during recombination, because of its effect on the recombination history of hydrogen.

ACKNOWLEDGMENTS

O.Z. thanks Christian Armendariz-Picon, Hans-Joachim Drescher and Emiliano Sefusatti for useful discussion. O.Z. is supported by the Deutscher Akademischer Austauschdienst. M.Z. and O.Z. are supported by NSF grants AST 0098606 and PHY 0116590 and by the David and Lucille Packard Foundation.

[1] X. Wang, M. Tegmark, and M. Zaldarriaga, Phys. Rev. D **65**, 123001 (2002).
[2] G. Efstathiou *et al.*, Mon. Not. R. Astron. Soc. **330**, L29 (2002).
[3] W.L. Freedman *et al.*, Astrophys. J. **553**, 47 (2001).
[4] A.G. Riess, Publ. Astron. Soc. Pac. **112**, 1284 (2000).
[5] W.L. Freedman, Int. J. Mod. Phys. A **1751**, 58 (2002).
[6] J.P. Kneller and G. Steigman, astro-ph/0210500.
[7] N. Arkani-Hamed, S. Dimopoulos, G. Dvali, and G. Gabadadze, hep-th/0209227.
[8] C. Deffayet, G.R. Dvali, and G. Gabadadze, Phys. Rev. D **65**, 044023 (2002).
[9] C. Deffayet, S.J. Landau, J. Raux, M. Zaldarriaga, and P. Astier, Phys. Rev. D **66**, 024019 (2002).
[10] J.M. O'Meara, D. Tytler, D. Kirkman, N. Suzuki, J.X. Prochaska, D. Lubin, and A.M. Wolfe, Astrophys. J. **552**, 718 (2001).
[11] S. Burles and D. Tytler, astro-ph/9712108.
[12] S. Burles and D. Tytler, astro-ph/9712109.
[13] S. Burles, K.M. Nollett, J.N. Truran, and M.S. Turner, Phys. Rev. Lett. **82**, 4176 (1999).
[14] K.A. Olive and E.D. Skillman, astro-ph/0007081.
[15] M. Peimbert, A. Peimbert, V. Luridiana, and M.T. Ruiz, astro-ph/0211497.
[16] K.A. Olive and D. Thomas, Astropart. Phys. **11**, 403 (1999).

[17] S.M. Carroll and M. Kaplinghat, Phys. Rev. D **65**, 063507 (2002).
[18] W. Hu and S. Dodelson, Annu. Rev. Astron. Astrophys. **40**, 171 (2002).
[19] P.J.E. Peebles, S. Seager, and W. Hu, Astrophys. J. Lett. **539**, L1 (2000).
[20] M. Kaplinghat, R.J. Scherrer, and M.S. Turner, Phys. Rev. D **60**, 023516 (1999).
[21] S. Landau, D. Harari, and M. Zaldarriaga, Phys. Rev. D **63**, 083505 (2001).
[22] S. Hannestad and R.J. Scherrer, Phys. Rev. D **63**, 083001 (2001).
[23] J.P. Uzan, hep-ph/0205340.
[24] A. Riazuelo and J. Uzan, Phys. Rev. D **66**, 023525 (2002).
[25] U. Seljak and M. Zaldarriaga, Astrophys. J. **469**, 437 (1996).
[26] W. Hu and N. Sugiyama, Phys. Rev. D **51**, 2599 (1995).
[27] C.P. Ma and E. Bertschinger, Astrophys. J. Lett. **434**, L5 (1994).
[28] P.J.E. Peebles, Astrophys. J. **153**, 1 (1968).
[29] M. Zaldarriaga and D.D. Harari, Phys. Rev. D **52**, 3276 (1995).
[30] N. Christensen, R. Meyer, L. Knox, and B. Luey, astro-ph/0103134.
[31] M. Tegmark, M. Zaldarriaga, and A.J. Hamilton, Phys. Rev. D **63**, 043007 (2001).
[32] Archeops Collaboration, A. Benoit, astro-ph/0210305.
[33] ACBAR Collaboration, C.L. Kuo *et al.*, astro-ph/0212289.
[34] J.E. Ruhl *et al.*, astro-ph/0212229.
[35] M. Tegmark and M. Zaldarriaga, Phys. Rev. D **66**, 103508 (2002).
[36] J. Kovac, E.M. Leitch, C.P. Carlstrom, and N.W. Holzapfel, Nature (London) **420**, 772 (2002).
[37] M. Zaldarriaga, D.N. Spergel, and U. Seljak, Astrophys. J. **488**, 1 (1997).
[38] J.B. Peterson *et al.*, astro-ph/9907276.
[39] D.B. Guenther, L.M. Krauss, and P. Demarque, Astrophys. J. **498**, 871 (1998).
[40] C.M. Will, Living Rev. Relativ. **4**, 4 (2001).
[41] K. Nordtvedt, Phys. Rev. D **169**, 1014 (1968).